Available online at www.sciencedirect.com
SCIENCE DIRECT®
Journal of Molecular Catalysis A: Chemical 224 (2004) 51–59
JOURNAL OF MOLECULAR CATALYSIS A: CHEMICAL
www.elsevier.com/locate/molcata

The fate of nitric oxide in its reaction with the 14-valence-electron planar species [(^{t}Bu$_2$PCH$_2$SiMe$_2$)$_2$N]RuCl☆

Lori A. Watson, Maren Pink, Kenneth G. Caulton*

Department of Chemistry, Indiana University, Bloomington, IN 47405, USA

Received 19 January 2004; received in revised form 1 June 2004; accepted 4 June 2004

Presented on the occasion of the 70th birthday of Prof J.J. Ziółkowski, in recognition of the great vision he has brought to the Institute of Chemistry in Wrocław.

Abstract

The reaction of NO with highly unsaturated, triplet spin state (PNP)Ru^{II}Cl ("PNP" = (^{t}Bu$_2$PCH$_2$SiMe$_2$)$_2$N) in benzene at 20 °C is reported. The reaction proceeds through three major intermediate species, ultimately forming [(PNP)Ru(NO)$_2^+$][Ru(NO)(OH)(NO$_2$)$_2$Cl$_2^-$], whose structure is determined by X-ray diffraction. The implications of PNP ligand loss, NO$_2^-$ production, and *partial* oxidation of ruthenium to Ru(III) (the anion above) are discussed, together with the observed oxygen transfer which represents NO disproportionation. The two NO ligands in the cation are chemically inequivalent (one bent, NO$^-$, and one linear, NO$^+$), features which are studied by density functional theory (DFT) geometry optimization. Two isomers of (PNP)Ru(NO)$_2$Cl, as well as (PNP)Ru(NO)Cl are evaluated as possible reaction intermediates by DFT geometry optimization.

Keywords: Nitric oxide; Disproportionation; Ruthenium; Homogeneous; DFT

1. Introduction

Reactions of nitric oxide, NO, are sometimes unselective. We consider that this can originate in the fact that NO, in spite of being "persistent" (stable) in the pure state, is a radical and thus will react by one-electron processes: hydrogen atom abstraction, and also initiation of radical chain processes. A subset of NO chemistry, transition metal coordination chemistry, also fits this generalization [1–7]. Reaction of NO with a reducible metal complex L_qM^n leads to a linear $L_qM^{(n-1)+}(NO^+)$ species by one-electron transfer *to* the metal. Reaction with an $S = \frac{1}{2}$ metal complex (e.g. L_nCo^{II}) leads to a bent nitrosyl complex, $Co^{III}(NO^{-1})$, by one-electron transfer *from* the metal to NO. Reaction with a 16-electron complex L_pM leads to a 1:1 adduct with the radical character located mainly on the nitrogen. It therefore shows the distinct reactivity characteristic of this new MNO species, but nevertheless radical reactivity. We have shown recently that such reactivity can be hydrogen atom abstraction [8], but it can also be reaction with excess NO (when present) [9] to ultimately catalyze a (disproportionation) reaction such as Eq. (1). In the presence of transition metal complexes, production of coordinated NO$_2$ (as NO$_2^-$), with liberation of N$_2$O, is a frequent result. In sum, NO

$$3NO \xrightarrow{[cat.]} N_2O + NO_2 \quad (1)$$

chemistry can be unselective and complex (i.e. multistep), and can proceed to convert an $S = \frac{1}{2}$ reagent into singlet spin state products.

We have reported [10] the synthesis of the molecule (PNP)RuCl (PNP = N(SiMe$_2$CH$_2$P^{t}Bu$_2$)$_2$), which is unusual in being (a) 4-coordinate Ru^{II}, (b) planar, and (c) having only

☆ Full details of the X-ray structure determination have been deposited in the form of the CIF file with Cambridge Crystallographic Data Centre, as CCDC 229386 available free from deposit@ccdc.cam.ac.uk.

* Corresponding author. Tel.: +1 812 855 4798; fax: +1 812 855 8300.
E-mail address: caulton@indiana.edu (K.G. Caulton).

1381-1169/$ – see front matter © 2004 Elsevier B.V. All rights reserved.
doi:10.1016/j.molcata.2004.06.035

14 valence electrons in contrast to the dictates of the 18-electron rule. As an even electron species, this might *not* display the kind of unusual chemistry described above with NO. However, the final unusual feature of (PNP)RuCl is that its six d electrons are not fully paired, as is generally the case for transition metals below the 3d series, but instead adopt an $S = 1$ state (*two* unpaired electrons). This report seeks to establish whether the favored reaction will couple triplet ground state (PNP)RuCl with two equivalents of NO, or whether the electron-rich character of (PNP)RuCl will lead to production of (coordinated, bent) NO^-, and how the resulting Ru(III) radical character might then evolve further, in secondary reactions. Because unsaturated, low coordinate species (e.g. (PNP)RuCl) generally react with very low activation energies, we can hope to study the reaction at mild temperature and controlled amounts of NO to intercept intermediates.

The goal of the present work is to define the reactivity of NO towards a uniquely highly unsaturated metal center but one which is electron-rich and so possesses the potential to transform to Ru^{III} or even Ru^{IV}. Relevant comparisons might be to 14 valence electron tetrahedral iron centers in the polymeric solid $[Fe(\mu\text{-}Cl)_2]_n$, or to $FeCl_2$(Lewis base)$_2$ species. The fundamental reactivity types have relevance to the catalytic disproportionation of NO, as well as conversion of NO by CO to more benign products, catalyzed by complexes of the late transition elements [11–16]. Complexes of NO have been studied earlier by Jezowska-Trzebiatowska and Ziółkowski [17].

2. Results

General. Some preliminary comments are useful concerning the utility of NMR spectroscopy in this system. Although (PNP)RuCl is paramagnetic (and shows no detectable ^{31}P NMR signals), its ^1H NMR spectrum shows resonances for all of its protons, and in a chemical shift range (+30 to −42 ppm; all signals outside the 0–10 ppm region) which makes it possible to detect its presence or absence after some addition of NO. Diamagnetic products *will* of course show ^{31}P NMR signals (but any paramagnetic products will be spectroscopically silent in the ^{31}P NMR spectrum). Unless otherwise stated, reactions were run and spectra recorded as follows: a benzene solution of (PNP)RuCl in an NMR tube was frozen, degassed, then a known number of millimoles of NO was added to the headspace over the frozen solution. The solution was brought to the melting point for a brief mixing time of gas and solution phases, then the solution was refrozen (−196 °C). Immediately prior to recording an NMR spectrum at 20 °C, the solution was thawed again. The time spent recording a spectrum at 20 °C was less than 10 min. Color changes are also useful in verifying altered solution composition.

Reaction progress.

(A) A 1:1 reaction of (PNP)RuCl (solutions are yellow) and NO in benzene forms a red solution immediately. The ^1H NMR spectrum shows an absence of (PNP)RuCl and no new paramagnetically shifted products formed. The strongest set of ^1H NMR peaks are those of P^{t}Bu(one triplet), CH_2 and $SiMe_2$ of a diamagnetic molecule, together with other much lower intensity peaks. The $^{31}P\{^1H\}$NMR spectrum at this time shows two singlets, one (70.6 ppm) approximately twice as abundant as the other (61.1 ppm). The simplicity of the ^1H NMR and the ^{31}P A_2 pattern at 70.6 ppm are consistent with a product of C_{2V} symmetry. After 1.5 h at room temperature both the ^1H and ^{31}P NMR spectra show additional new peaks (three new ^{31}P signals), but they are still weaker than those observed earlier. After 2 days, there was little additional change in the NMR spectra, but the solution color was now yellow-green.

(B) To establish the impact of additional (excess) NO, the above experiment was repeated with a Ru:NO ratio of 1:1.8. The solution became green immediately. The ^{31}P NMR showed five signals, of different intensities, only one of which was that in (A); one new product has chemical shift 80.4 ppm. The ^{31}P NMR spectrum changed little over the next 2 days, although after only 3 h, the solution was orange. After 2 weeks, red crystals formed from the benzene solution. The content of these crystals was established as $[(PNP)Ru(NO)_2][Ru(NO)(OH)Cl_2(NO_2)_2]$ by X-ray diffraction (Tables 1 and 2).

Structure. The $(PNP)Ru(NO)_2^+$ cation (Fig. 1) is mirror symmetric, with Ru, both NO, and the amide nitrogen lying in the crystallographic mirror plane. The coordination geometry is square pyramidal, and the two nitrosyl ligands are chemically inequivalent [18–20]. N3/O3 is a bent nitrosyl ("NO^-") at the apical site in

Table 1
Crystal data and structure refinement for $[(PNP)Ru(NO)_2][Ru(NO)(OH)Cl_2(NO_2)_2]$

Empirical formula	$C_{22}H_{53}Cl_2N_6O_8P_2Ru_2Si_2$
Formula weight	920.86
Crystal color, shape, size	Red block, 0.20 mm × 0.12 mm × 0.10 mm
Temperature	133(2) K
Wavelength	0.71073 Å
Crystal system, space group	Orthorhombic, *Pnma*
Unit cell dimensions	$a = 10.0852(12)$ Å, $\alpha = 90°$; $b = 13.7681(17)$ Å, $\beta = 90°$; $c = 28.198(4)$ Å, $\gamma = 90°$
Volume	3915.3(8) Å^3
Z	4
Density (calculated)	1.562 Mg/mm^3
Absorption coefficient	1.097 mm^{-1}
Goodness-of-fit on F^2	1.024[a]
Final R indices $[I > 2\sigma(I)]$	R1 = 0.0633[b], wR2 = 0.1658[c]
R indices (all data)	R1 = 0.0701[b], wR2 = 0.1720[c]
Largest diffraction peak and hole	3.282 and −2.085 e Å^{-3}

[a] Goodness-of-fit $= [\sum[w(F_o^2 - F_c^2)^2]/(N_{observns} - N_{params})]^{1/2}$, all data.
[b] $R1 = \sum(|F_o| - |F_c|)/\sum|F_o|$.
[c] $wR2 = [\sum[w(F_o^2 - F_c^2)^2]/\sum[w(F_o^2)^2]]^{1/2}$.

Table 2
Bond lengths (Å) and angles (°) for one cation and the anion in $[(PNP)Ru(NO)_2][Ru(NO)(OH)(NO_2)_2Cl_2]$

Cation	X-ray	DFT	Anion	
Ru1—N2	1.760(6)	1.796	Ru2—N4	1.750(10)
Ru1—N3	1.910(6)	1.947	Ru2—N5	2.02(2)
Ru1—N1	2.046(6)	2.046	Ru2—O1	2.094(8)
Ru1—P1	2.45(2)	2.433	Ru2—N7	2.19(4)
N1—Si1	1.700(5)	1.759	Ru2—N8	2.228(11)
O2—N2	1.157(9)	1.151	Ru2—Cl6	2.344(4)
O3—N3	1.174(9)	1.162	Ru2—Cl5	2.413(5)
N2—Ru1—N3	97.6(3)	101.4	O4—N4	1.106(13)
N2—Ru1—N1	165.3(3)	158.7	O5A—N5	1.231(17)
N3—Ru1—N1	97.0(3)	99.8	O5B—N5	1.264(17)
N2—Ru1—P1	90.4(4)	94.5	O7A—N7	1.21(2)
N3—Ru1—P1	97.6(4)	95.9	O7B—N7	1.191(19)
N1—Ru1—P1	87.7(4)	83.4	O8A—N8	1.169(11)
P1—Ru1—P1#1	164.5(7)	163.6	O8B—N8	1.145(13)
Si1—N1—Si1B	116.7(4)	116.3	N4—Ru2—N8	92.2(4)
Si1—N1—Ru1	127.6(2)	121.9	N5—Ru2—N8	86.1(3)
O2—N2—Ru1	178.1(7)	169.7	O1—Ru2—N8	82.9(3)
O3—N3—Ru1	129.0(6)	126.3	N7—Ru2—N8	96.4(9)
			N4—Ru2—Cl6	95.4(3)
			N5—Ru2—Cl6	92.67(17)
			O1—Ru2—Cl6	89.58(10)
			N7—Ru2—Cl6	84.2(9)
			N8—Ru2—Cl6	172.5(3)
			N4—Ru2—Cl5	92.6(4)
			O1—Ru2—Cl5	88.7(3)
			N7—Ru2—Cl5	175.7(9)
			N8—Ru2—Cl5	87.6(3)
			Cl6—Ru2—Cl5	91.66(12)
			N4—Ru2—N5	96.4(6)
			N4—Ru2—O1	174.9(4)
			N5—Ru2—O1	84.9(6)
			N4—Ru2—N7	88.9(8)
			N5—Ru2—N7	174.1(10)
			O1—Ru2—N7	90.1(8)
			O4—N4—Ru2	176.2(11)

the square pyramid; the linear nitrosyl, a strong π-acid, lies *trans* to the π-donor amide, and thus strengthens mutual bonding by a push/pull interaction among the amide lone pair, a filled Ru d_π orbital, and the linear nitrosyl π^* orbital. The Ru/N bond lengths reflect this in

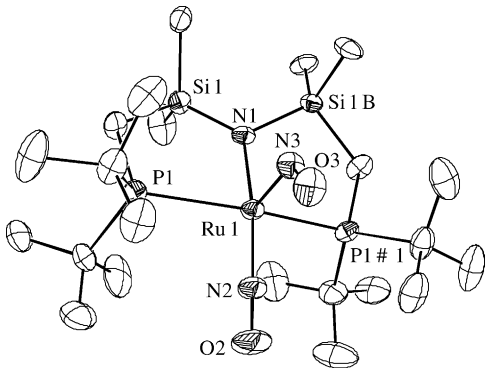

Fig. 1. ORTEP view (50% probability ellipsoids) of the cation $[(^tBu_2PCH_2SiMe_2)_2N]Ru(NO)_2^+$, showing selected atom labeling.

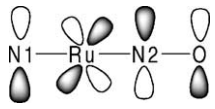

being short to N1 (compared to a single bond) and to N2 (compared to other Ru/nitrosyl distances). The Ru–N3–O3 angle 129.0(6)°, is consistent with sp^2 hybridization at N3, and thus a lone pair on that nitrogen. A bent nitrosyl is a strong *trans* director (i.e. NO^- is a strong σ-donor to Ru), and thus there is no ligand *trans* to N3/O3, in spite of the Ru in the cation being formally unsaturated (barring N1 → Ru/π donation). The formal metal oxidation state is Ru(II), which is unchanged from that in the reagent (PNP)RuCl. This compound shows a (linear) NO^+ stretching frequency of 2004 cm^{-1} which is assigned to ν_{NO} of the basal nitrosyl in the cation.

The accompanying anion (Fig. 2) shows an octahedron with a linear NO *trans* to hydroxide, two *cis* NO_2^- ligands, and two *cis* chloride ligands. The metal in $Ru(NO^+)(OH)(NO_2)_2Cl_2^{-1}$ thus has oxidation state +3, a common one for ruthenium nitrosyls [21]. The Ru–NO

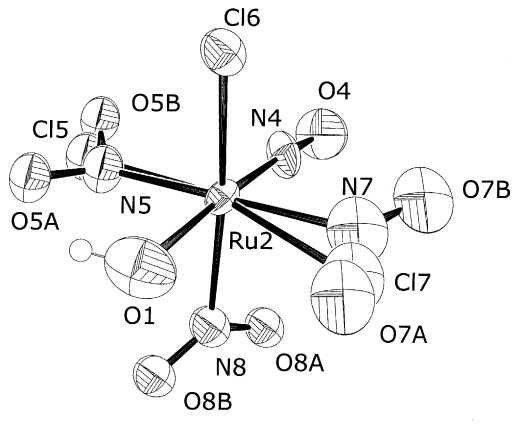

Fig. 2. ORTEP view (50% probability ellipsoids) of the anion $Ru(NO)(OH)(NO_2)_2Cl_2^-$. Only the disorder of C15, C17 and their associated NO_2 groups is shown. The hydroxide proton has been place in an idealized position.

distance, 1.750(10) Å, is comparable to that involving the linear NO in the cation. The second observed NO stretching frequency, 1875 cm^{-1}, is lower due to increased back donation from this Ru(III) center carrying many anionic ligands. The nitro ligands are N-bound to Ru, and each is *trans* to a chloride. There are no exceptional structural features in the anion.

(C) We attempted to detect a primary product, and so better understand the early evolution of the reaction by sequential dosing of increasing amounts of NO into a benzene solution of (PNP)RuCl, beginning with an amount consciously chosen to be substoichiometric (to avoid, to the extent possible, conversion of the primary product by a second molecule of NO; this can succeed only if the rate of the second step is slower than the rate of the first step).

(1) 0.25 equiv. NO: The solution color is yellow-green, unreacted (PNP)RuCl remains (^{1}H NMR evidence), and the major product by ^{31}P NMR is the 70.6 ppm species seen in (A) above. This 1:4 NO:Ru ratio is thus established to be sub-stoichiometric, as anticipated.

(2) 0.5 equiv. NO: The solution color is green, no (PNP)RuCl can be detected, and the 70.6 ppm peak is now accompanied by a second peak, at 61.0 ppm.

(3) 0.75 equiv. NO: The solution color is a duller green, and the 70.6 and 61.0 ppm peaks are accompanied by a third singlet (80.4 ppm), seen above in (B).

(4) 1.0, 1.5, 2.0, and 3.0 NO:Ru ratios: The solution color changes progressively towards olive, then yellow-brown, and the ^{31}P NMR shows a progressive decline in the 70.6 ppm peak, but the 80.6 and 61.0 singlets remain relatively unchanged and dominant. At a ratio of 3.0, the solution is orange-brown.

In sum, the system can be described with three major species (Eq. (2)), designated by their $\delta(^{31}P)$ values:

$$(PNP)RuCl \xrightarrow{NO} 70.6 \xrightarrow{NO} 61.0 \text{ and } 80.6 \qquad (2)$$

Reactivity toward N_2O. The presence of NO_2^- ligands in the isolated salt implies the co-production of some products, which are nitrogen-rich compared to the 1:1 ratio in reagent NO. For example (Eq. (1)), N_2O might be anticipated. This molecule has shown itself to be a very poor ligand, but it is of interest as a potential oxygen atom transfer reagent, with N_2 as a co-product [22–25]. We therefore tested for possible secondary reactions resulting from one possible co-product by adding excess N_2O (1 atm) to (PNP)RuCl in benzene at 23 °C. There was no color change and ^{31}P NMR confirmed the absence of reaction products. Even after 22 h, a time too long to be relevant to our NO reaction studies, 80% of (PNP)RuCl remained unchanged. These results also show that a product like **1** is not efficiently formed, in spite of the electron-rich character of (PNP)RuCl; N_2O is not an effective O-atom transfer reagent in this case.

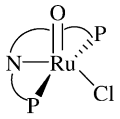

1

Structure from density functional calculations.

(a) *The final product*. We have performed a DFT geometry optimization of the species $(PNP^H)Ru(NO)_2^+$, where PNP^H is $(H_2PCH_2SiH_2)_2N$. Starting geometries for the optimizations were near-C_{2V} in which both RuNO units were (a) linear or (b) bent *outwards*. Each ultimately converged to a "linear + bent" structure and square pyramidal geometry, in satisfactory agreement with the experimentally determined structure (Fig. 3 and Table 2).Starting the geometry optimization from a near-C_{2V} structure where both RuNO units were bent *towards* one another (**2′**) led to a different minimum energy structure (**2**) with one bent NO (i.e. NO^-) and the second NO bound η^2 (i.e. bidentate, through both N and O) to Ru.

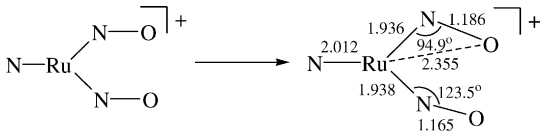

2' **2**

This can be considered as an η^2-(NO^+) adduct of a neutral (PNP)Ru(NO^-) species, the latter thus being analogous to (PNP)RuCl. This η^2-NO structure, while unusual, has been discussed several times recently [26]. It is calculated to lie +18 kcal/mol (ΔE + ZPE) above the observed structure (Fig. 1) and is therefore not mechanistically relevant.

(b) *The 1:1 adduct*. The optimized geometry of the primary product, a 1:1 adduct of uncharged (PNP)RuCl and NO, was calculated as a spin doublet. It contains a linear NO at a basal site in a square pyramidal coordination geometry (Fig. 4). Chloride is apical, *trans* to the empty coordi-

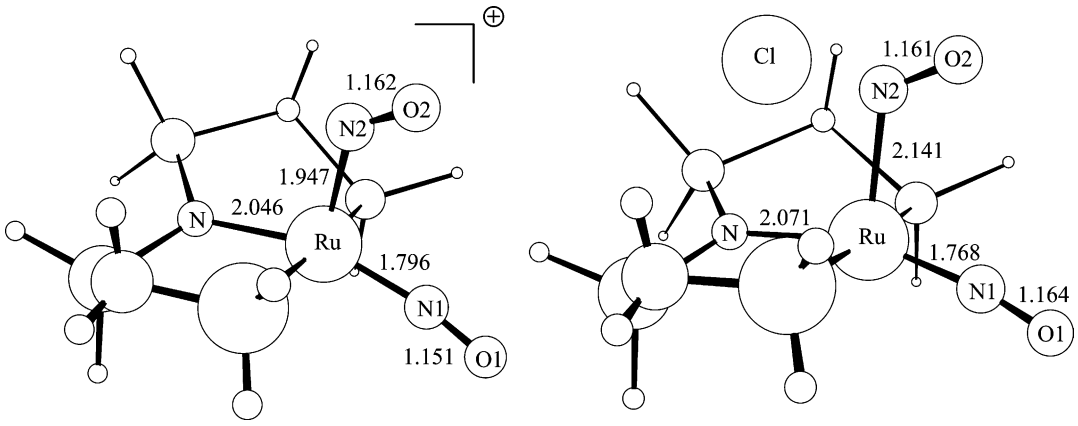

Fig. 3. DFT geometry-optimized structures of $(PNP^H)Ru(NO)_2^+$ (left) and its ion pair with Cl^- (right), showing selected atom labelling and selected bond lengths.

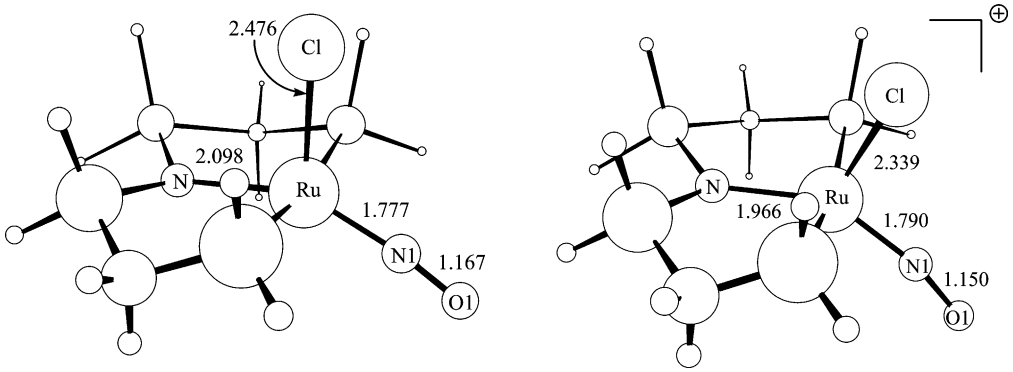

Fig. 4. Minimum DFT energy structures of $(PNP^H)Ru(NO)Cl$ (left) and $(PNP^H)Ru(NO)Cl^+$ (right).

nation site. The bond dissociation enthalpy (Eq. (3)) is 30.4 kcal/mol which indicates strong binding (large K_{eq}). The spin density in

$$(PNP^H)RuCl(NO) \rightarrow (PNP^H)RuCl + NO \quad (3)$$

$(PNP^H)Ru(NO)Cl$ is 68% on Ru, 13% on Cl, and 10% on the amide nitrogen. The geometry of the singlet cation $(PNP^H)Ru(NO)Cl^+$ was calculated for comparison (Fig. 4), to evaluate the character of the orbital to which the last electron is added. $(PNP^H)Ru(NO)Cl^+$ is also square pyramidal with nitrosyl in a basal site. The major changes upon 1 e^- reduction are lengthening of Ru-amide (by 0.132 Å) and Ru–Cl (by 0.137 Å), so this frontier orbital is antibonding in both these bonds. In particular, the singly occupied orbital in $(PNP^H)Ru(NO)Cl$ is repulsive towards the amide N/Ru π donation. An examination of the SOMO wave function (Fig. 5) confirms this conclusion from the spin densities: the orbital is composed of the amide nitrogen p_π AO and a hybrid of the d_{z2} orbital with the d_{xz} orbital, the d orbital mixing being due to the distortion of the chlorine from the NP_2Ru plane. There is significant participation by that chlorine p orbital which lies along the Ru–Cl bond (i.e. a p_σ orbital there) and there is *negligible* participation by the nitrosyl π^* orbital (4% spin density on each of N and O).

(c) *Dissociation of chloride*. It is clear that the ruthenium which has lost its PNP ligand is electrophilic, and thus can accept chloride, as well as bind additional NO and be a site for NO disproportionation. As another possible mechanism for chloride transfer, we have attempted to

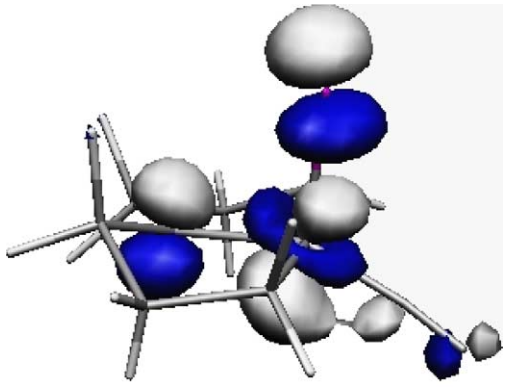

Fig. 5. Wave function of singly occupied molecular orbital of $(PNP^H)Ru(NO)Cl$.

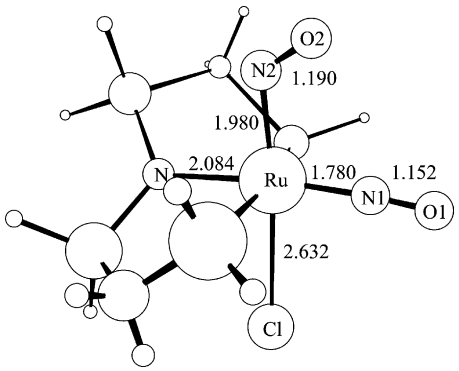

Fig. 6. Minimum DFT energy structure of the isomer of $(PNP^H)Ru(NO)_2Cl$ with (weak) bonding of Cl *trans* to the bent nitrosyl.

evaluate the RuCl bond in a potential *early* intermediate $(PNP^H)Ru(NO)_2Cl$, where *two* NO molecules have added to the opposite faces of planar 14-valence-electron $(PNP^H)RuCl$. DFT geometry optimization of this species revealed that such a complex is not stable, but instead *spontaneously dissociates chloride*. Starting from a near-C_{2V} geometry where the Ru–Cl vector (initial distance 2.36 Å) lies between the two linear nitrosyls, the Ru–Cl distance continuously lengthens to 4 Å, at which point the optimization was terminated. As the chloride departs, the $Ru(NO)_2$ substructure begins to differentiate the two NO ligands to the linear and bent forms found in the more stable structure of the cation $(PNP)Ru(NO)_2^+$. However, beginning from geometry **3**, a stationary point was found. This second isomer of $(PNP^H)Ru(NO)_2Cl$ (Fig. 6), formed

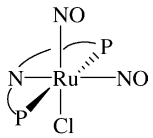

3

from approach of NO to the open coordination site of $(PNP^H)Ru(NO)Cl$ in Fig. 4, is an energy minimum, but the binding enthalpy for this second NO to $(PNP^H)Ru(NO)Cl$ is only 17.4 kcal/mol and the ΔG°_{298} for its formation is only −4.7 kcal/mol. The *structure* of this adduct differs in only minor ways from the chloride loss product, $(PNP^H)Ru(NO)_2^+$ (compare Figs. 3 and 6), which is consistent with the fact that the Ru–Cl distance in the molecule is exceptionally long, 2.632 Å, and the weak binding of Cl seen from the enthalpy for going from the molecular species (Fig. 6) to the ion pair (Fig. 3), +17.4 kcal/mol. This ion pair of $(PNP^H)Ru(NO)_2^+$ with chloride (Fig. 3), where chloride was initially located above the NSi_2 plane and *syn* to the bent NO, was intended to mimic the product of Cl^- loss in benzene. The stationary point determined for the ion pair has the $(PNP)Ru(NO)_2^+$ substructure only mildly perturbed from that in free $(PNP^H)Ru(NO)_2^+$. The Ru/Cl separation in the ion pair is 3.581 Å. The biggest change from $(PNP^H)Ru(NO)_2^+$ is a movement of the bent NO slightly away from the metal (Ru–N lengthens by 0.194 Å and the Ru–N–O angle decreases by 6.6°). All together, these studies suggest that Cl^- is actively displaced by the binding of the second NO, and that the resulting $(PNP^H)Ru(NO)_2^+$ structure is robust to external perturbation by a reagent as nucleophilic as Cl^-. In summary regarding mechanism, this establishes that addition of the second NO to $(PNP^H)RuCl$ *displaces* Cl^- rather than simply adding to the monoadduct. Although some electrophile is necessary to accept Cl^- in the low dielectric (benzene) medium, the electrophile is not needed for thermodynamic driving force to break the Ru–Cl bond.

3. Discussion

Although spectroscopy, crystallography and computational evaluation of potential intermediates have helped to define this reaction system, its complexity has frustrated full understanding. The ^{31}P NMR chemical shifts observed for reaction intermediates are sufficiently close together that a structure that involves a phosphine oxide, $R_2R'P{=}O$ is excluded; conversion from P^{III} to P^V normally moves a chemical shift to a more positive value by 40–50 ppm. The 70.6 ppm species (Eq. (2)) cannot be a 1:1 product, since that would have an odd number of electrons (thus no ^{31}P NMR signal). Because its ^1H and ^{31}P NMR show it to have C_{2V} symmetry, we assign it as **4**.

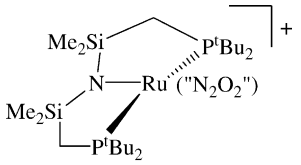

4

The ^1H NMR intensities require that the "N_2O_2" unit, which must donate a total of four electrons to satisfy the 18-electron rule [27], must be two-fold symmetric, either in the ground state or by a dynamic process rapid on the ^1H NMR time scale. If it contains an N/N bond, it could be a precursor to N_2O. The other two products ($\delta(^{31}P) = 61.0$ and 80.6) are more robust to increasing excess NO, and it is thus likely that they lead to the crystallographically characterized product. Their diminished reactivity towards free NO suggests that they contain linear NO (lacking a lone pair, these are usually relatively resistant to oxidation by excess NO), as well as the obviously oxidation resistant NO_2 ligands. Although the anion in the crystalline product lacks any PNP ligand, the fate of this ligand remains unknown, and it does not appear as any single high yield product by ^{31}P NMR studies. One way that it might be removed from ruthenium is by nitrosylation (i.e. oxidation) of the electron-rich amide nitrogen, to give the nitrosoamine **5**. It must also be recognized that one fate

of the oxygen of NO might be to bond to Si, by cleaving a Si–C or Si–N bond.

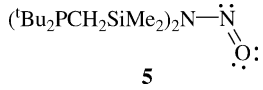

5

Efforts to avoid excess NO and to combine the reagents under mild temperature conditions have failed to reveal the primary product or to achieve even a secondary product with high yield/selectivity. This may reflect (a) the bifunctional (i.e. 14 valence electrons) character of (PNP)RuCl (leading rapidly to 2:1 NO:Ru stoichiometry) and (b) the fact that the primary product ("(PNP)Ru(NO)Cl") is a radical, and that there is no good radical quencher in this system *except* more NO. The latter, because it encourages formation of a "N_2O_2" ligand, promotes oxygen transfer and formation of coordinated NO_2. There is no evidence for a significant amount of radical degradation of the PNP ligand since this would make the two chelate "arms" inequivalent and produce an AB $^{31}P\{^1H\}$ NMR pattern, which was not observed.

The characterized product, because its cation contains an NO^+ and NO^- ligand, is still a complex of Ru(II), the initial reagent oxidation state, so this fraction of the consumed ruthenium has been a mediator of neutral NO *disproportionation* without undergoing redox change itself. The companion complex anion, however, is in a higher oxidation state, so oxidation of Ru has occurred. The *loss* of Cl^- in the characterized cation suggests the participation by some (undetected) electrophile (either oxidized ruthenium – note the two chloride per Ru in the characterized anion – or by NO^+, forming ClNO as an intermediate). H^+ demands consideration as an acid facilitating Ru–Cl cleavage, but our reaction solvent (arenes) makes this unlikely. The kinetic facility of these reactions, under even our room temperature conditions, is consistent with participation by Lewis acids and/or radicals. However, the discovery by DFT that one structure of $(PNP^H)Ru(NO)_2Cl$ spontaneously dissociates Cl^- means that Ru–Cl bond heterolysis is barrierless and thus a Lewis acid is not actually required. Given the poor material balance we could achieve, the question of whether the OH ligand derives its oxygen from reagent NO cannot be answered with certainty.

The average ratio of N to Ru in $[(PNP)Ru(NO)_2][Ru(NO)(OH)Cl_2(NO_2)_2]$ is 2.5:1, and thus this is clearly a product of excess NO. Even at the lowest NO:Ru ratios employed here, the primary product detected apparently has two NO per Ru. Cases where two NO donate a total of four valence electrons are known, and can have equivalent NO ligands, rather than one bent (1e donor) and one linear (3e donor) [27]. The facile consumption of *two* NO by (PNP)RuCl surely results from it being the unique reagent studied to-date with only 14 valence electrons, and thus access to two empty *orbitals*. It has been shown earlier [9] that free NO can oxidize coordinated NO by oxo transfer. If indeed the bis-NO adduct binds a third NO ligand (i.e. the *stoichiometry* of Eq. (1)), then oxidation can be initiated by substructure **6** or **7**. The production of Ru(III) follows from the fact that one product of Eq. (1), NO_2, needs one electron to become an NO_2^- ligand on ruthenium.

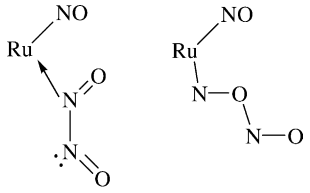

6 **7**

4. Experimental

General considerations. All manipulations were performed using standard Schlenk techniques or in an argon filled glovebox unless otherwise noted. Solvents were distilled from Na/benzophenone, CaH_2, or 4 Å molecular sieves, degassed prior to use, and stored in air-tight vessels. (PNP)RuCl was prepared according to published procedures [10]. All other reagents were used as received from commercial vendors. ^1H NMR chemical shifts are reported in ppm relative to protio impurities in the deuterated solvents. ^{31}P NMR spectra are referenced to external standards of 85% H_3PO_4 (at 0 ppm). NMR spectra were recorded with a Varian Gemini 2000 (300 MHz ^1H; 121 MHz ^{31}P), a Varian Unity Inova instrument (400 MHz ^1H; 162 MHz ^{31}P), or a Varian Unity Inova instrument (500 MHz ^1H). Only one example of the execution of reaction is given, it being typical of all experiments.

$(PNP^{tBu})RuCl + 1.8\,NO$: (PNP)RuCl (10.2 mg, 0.0179 mmol) was dissolved in approximately 0.5 mL C_6D_6. Head space gases were removed via multiple freeze–pump–thaw cycles. 1.8 equiv. of NO was added to the frozen solution via standard gas line techniques. The solution was warmed to thaw, mixed quickly, and then refrozen at 77 K. The solution was thawed immediately prior to NMR measurements, which were taken at 25 °C. $^{31}P\{^1H\}$ NMR (162 MHz, C_6D_6, 25 °C): δ 80.4 (s), 64.3 (s), 62.5 (s), 61.6 (s), and 60.9 (s) among other signals of lower intensity. The J-Young tube was placed in an argon filled glovebox. After 2 weeks crystals suitable for X-ray diffraction had formed.

X-ray structure determination. The data collection (SMART6000(Bruker)) was carried out at 133(2) K using Mo Kα radiation (graphite monochromator) with a frame time of 15 s and a detector distance of 5.0 cm. A randomly oriented region of reciprocal space was surveyed to the extent of a sphere. Four major sections of frames were collected with 0.30° steps in ω at four different ϕ settings and a detector position of −43° in 2θ. An additional set of 80 frames was collected in order to medal decay. Data to a resolution of 0.84 Å were considered in the reduction. Final cell constants (Table 1) were calculated from the *xyz* centroids of

6791 strong reflections from the actual data collection after integration (SAINT) [28]. The intensity data were corrected for absorption (SADABS) [29]. The space group *Pnma* was determined based on intensity statistics and systematic absences. The structure was solved using SIR-92 [30] and refined with SHELXL-97 [31]. A direct-methods solution was calculated which provided most non-hydrogen atoms from the E-map. Full-matrix least squares/difference Fourier cycles were performed which located the remaining non-hydrogen atoms. All non-hydrogen atoms were refined with anisotropic displacement parameters except for O8b. Atom O5b was restrained so that its U_{ij} components approximate to isotropic behavior. A set of restraints and constraints was used for the anion. The hydrogen atoms were placed in ideal positions and refined as riding atoms with relative isotropic displacement parameters. The remaining electron density is located in the vicinity of the Ru atoms; peak and hole are of the same magnitude. The composition was found to be $[Ru(PNP)(NO)_2][Ru(NO)(OH)Cl_2(NO_2)_2]$ with half the formula unit comprising the asymmetric unit. Both anion and cation are disordered. The entire PNP ligand of the cation is disordered such that silicon is located below or above the Ru, N1, P, P′ plane. The ruthenium atom is disordered to opposite sides of a mirror plane in the anion. In the octahedral anion, two *trans* positions are occupied by NO^+ and OH^- and in the remaining four positions, Cl^- and NO_2^- are statistically disordered with each other. The nature and connectivity of the ligands in the anion and their site occupancies were determined based on refined site occupancies, temperature factors, and by comparison to typical bond lengths [32]. In the final refinement, site occupancies were fixed. Only the hydroxide oxygen and one nitro N and O lie on a crystallographic mirror plane. All other ligands have fractional occupancy, related in part to Ru lying 0.35 Å off the mirror plane.

Computational details: All calculations were performed with the Gaussian'98 package [33] at the B3PW91 [34–37] level of theory. Basis sets used included LANL2DZ for Ru, Cl and Si, 6-31G* for C, N and O, and 6-31G** for all hydrogens [38]. The basis set LANL2DZ is the Los Alamos National Laboratory ECP plus a double zeta valence on Ru, P, Cl and Si [39–41]; additional d polarization functions [42] were added to all phosphorus, chlorine and silicon atoms in all DFT calculations. All optimizations were performed with C_1 symmetry and all minima were confirmed by analytical calculation of frequencies, which were also used to compute zero point energy corrections without scaling.

Acknowledgments

This work was supported by the National Science Foundation. LAW also thanks NSF for a predoctoral fellowship and Indiana University for a Wells Fellowship.

References

[1] G.R. Richter-Addo, P. Legzdins, Metal Nitrosyls, Oxford University Press, New York, 1992.
[2] K.G. Caulton, Coord. Chem. Rev. 14 (1975) 317.
[3] D. Gwost, K.G. Caulton, J. Chem. Soc., Chem. Commun. (1973) 64.
[4] D. Gwost, K.G. Caulton, Inorg. Chem. 12 (1973) 2095.
[5] K.G. Caulton, J. Am. Chem. Soc. 95 (1973) 4076.
[6] C.B. Ungermann, K.G. Caulton, J. Am. Chem. Soc. 98 (1976) 3862.
[7] G.B. Richter-Addo, P. Legzdins, J. Burstyn, Chem. Rev. 102 (2002) 857.
[8] A.V. Marchenko, A.N. Vedernikov, D.F. Dye, M. Pink, J.M. Zaleski, K.G. Caulton, Inorg. Chem. 43 (2004) 351.
[9] D. Gwost, K.G. Caulton, Inorg. Chem. 13 (1974) 414.
[10] L.A. Watson, O.V. Ozerov, M. Pink, K.G. Caulton, J. Am. Chem. Soc. 125 (2003) 8426.
[11] J. Reed, R. Eisenberg, Science 184 (1974) 568.
[12] R. Eisenberg, C.D. Meyer, Acc. Chem. Res. 8 (1975) 26.
[13] C.D. Meyer, R. Eisenberg, J. Am. Chem. Soc. 98 (1976) 1364.
[14] D.E. Hendriksen, R. Eisenberg, J. Am. Chem. Soc. 98 (1976) 4662.
[15] D.E. Hendriksen, C.D. Meyer, R. Eisenberg, Inorg. Chem. 16 (1977) 970.
[16] K.J. Stanger, R.J. Angelici, J. Mol. Catal. A: Chem. 207 (2004) 59.
[17] B. Jezowska-Trzebiatowska, J. Ziółkowski, Z. Chem. 3 (1963) 333.
[18] R. Eisenberg, C.G. Pierpont, J. Am. Chem. Soc. 93 (1971) 4905.
[19] C.G. Pierpont, D.G. Van Derveer, W. Durland, R. Eisenberg, J. Am. Chem. Soc. 92 (1970) 4760.
[20] C.G. Pierpont, R. Eisenberg, Inorg. Chem. 11 (1972) 1088.
[21] A.J. Schultz, R.L. Henry, J. Reed, R. Eisenberg, Inorg. Chem. 13 (1974) 732.
[22] G.A. Vaughan, P.B. Rupert, G.L. Hillhouse, J. Am. Chem. Soc. 109 (1987) 5538.
[23] G.A. Vaughan, G.L. Hillhouse, R.T. Lum, S.L. Buchwald, A.L. Rheingold, J. Am. Chem. Soc. 110 (1988) 7215.
[24] G.A. Vaughan, G.L. Hillhouse, A.L. Rheingold, J. Am. Chem. Soc. 112 (1990) 7994.
[25] P.T. Matsunaga, J.C. Mavropoulos, G.L. Hillhouse, Polyhedron 14 (1995) 175.
[26] P.N. Coppens, I. Kovalevsky, Chem. Rev. 102 (2002) 861.
[27] Y.S. Yu, R.A. Jacobson, R.J. Angelici, Inorg. Chem. 21 (1982) 3106.
[28] SAINT 6.1, Bruker Analytical X-ray Systems, Madison, WI.
[29] R. Blessing, Acta Crystallogr A 51 (1995) 33.
[30] A. Altomare, G. Cascarno, C. Giacovazzo, A. Gualardi, J. Appl. Crystallogr. 26 (1993) 343.
[31] SHELXTL-Plus, Bruker Analytical X-ray Systems, Madison, WI.
[32] International Tables for Crystallography, vol. C, 2nd ed., Kluwer Academic Publishers, 1999.
[33] M.J. Frisch, G.W. Trucks, H.B. Schlegel, G.E. Scuseria, M.A. Robb, J.R. Cheeseman, V.G. Zakrzewski, J. Montgomery, R.E. Stratmann, J.C. Burant, S. Dapprich, J.M. Millam, A.D. Daniels, K.N. Kudin, M.C. Strain, O. Farkas, J. Tomasi, V. Barone, M. Cossi, R. Cammi, B. Mennucci, C. Pomelli, C. Adamo, S. Clifford, J. Ochterski, G.A. Petersson, P.Y. Ayala, Q. Cui, K. Morokuma, D.K. Malick, A.D. Rabuck, K. Raghavachari, J.B. Foresman, J. Cioslowski, J.V. Ortiz, A.G. Baboul, B.B. Stefanov, G. Liu, A. Liashenko, P. Piskorz, I. Komaromi, R. Gomperts, R.L. Martin, D.J. Fox, T. Keith, M.A. Al-Laham, C.Y. Peng, A. Nanayakkara, C. Gonzalez, M. Challacombe, P.M.W. Gill, B. Johnson, W. Chen, M.W. Wong, J.L. Andres, M. Head-Gordon, E.S. Replogle, J. Pople, Gaussian'98, Revision A.7, 1998.
[34] A.D. Becke, Phys. Rev. A 38 (1988) 3098.

[35] A.D. Becke, J. Chem. Phys. 98 (1993) 1372.
[36] A.D. Becke, J. Chem. Phys. 98 (1993) 5648.
[37] J.P. Perdue, Y. Wang, Phys. Rev. B. 45 (1991) 13244.
[38] P.C. Hariharan, J.A. Pople, Theor. Chim. Acta 28 (1973) 213.
[39] P.J. Hay, W.R. Wadt, J. Chem. Phys. 82 (1985) 270.
[40] W.R. Wadt, P.J. Hay, J. Chem. Phys. 82 (1985) 284.
[41] P.J. Hay, W.R. Wadt, J. Chem. Phys. 82 (1985) 299.
[42] A. Höllwarth, M. Böhme, S. Dapprich, A.W. Ehlers, A. Gobbi, V. Jonas, K.F. Köhler, R. Stegmann, A. Veldkamp, G. Frenking, Chem. Phys. Lett. 208 (1993) 237.